

Physically Adversarial Attacks and Defenses in Computer Vision: A Survey

Xingxing Wei, Bangzheng Pu, Jiefan Lu, and Baoyuan Wu

Abstract—Although Deep Neural Networks (DNNs) have been widely applied in various real-world scenarios, they are vulnerable to adversarial examples. The current adversarial attacks in computer vision can be divided into digital attacks and physical attacks according to their different attack forms. Compared with digital attacks, which generate perturbations in the digital pixels, physical attacks are more practical in the real world. Owing to the serious security problem caused by physically adversarial examples, many works have been proposed to evaluate the physically adversarial robustness of DNNs in the past years. In this paper, we summarize a survey versus the current physically adversarial attacks and physically adversarial defenses in computer vision. To establish a taxonomy, we organize the current physical attacks from attack tasks, attack forms, and attack methods, respectively. Thus, readers can have a systematic knowledge about this topic from different aspects. For the physical defenses, we establish the taxonomy from pre-processing, in-processing, and post-processing for the DNN models to achieve a full coverage of the adversarial defenses. Based on the above survey, we finally discuss the challenges of this research field and further outlook the future direction.

Index Terms—Physically adversarial attacks, Physically Adversarial defenses, AI safety, Deep learning, Computer vision.

1 INTRODUCTION

Deep Neural Networks (DNNs) have achieved impressive performance in Computer Vision (CV) and Natural Language Processing (NLP), and thus are widely applied in businesses and industries, such as mobile payment [38], autonomous driving [6], surveillance [4], robotics [101], and medical diagnosis [10], etc. However, the potential crises hide behind the prosperity. Szegedy et al. [49] discover that only a tiny perturbation can overthrow the correct predictions of state-of-the-art DNN models. This malicious behavior is defined as the Adversarial Attacks and the manipulated image is called the Adversarial Example. After that, the effectiveness of adversarial examples has been proved in different CV tasks, which mainly contain image classification [84], semantic segmentation [55], object detection [107], object tracking [27], motion detection [90] etc. Moreover, some researches [81], [165] also demonstrate the vulnerability of DNNs in theory.

In computer vision, according to the implementary domain, adversarial attacks can be distinguished to digital attacks and physical attacks. Digital attacks denote performing attacks in the digital pixels after the camera imaging, and physical attacks denote performing attacks on the physical objects before the camera imaging. Although digital attacks (like PGD [86], MI-FGSM [35], C&W [16], and Deepfool [92] etc.) have performed well against DNN models, they are difficult to be implemented in the real world. Because digital perturbations are usually global and inconspicuous, which are hard to be captured clearly by the camera. These drawbacks urge researchers to investigate more practical attack manners in the physical world.

For that, many physically adversarial attacks have been reported in autonomous driving [14, 43, 85, 118, 19, 69, 7, 152, 39, 145, 128], face recognition [114, 85, 98, 116, 113, 142], security surveillance [123, 140, 144, 62, 61, 135, 33, 130, 60]. These works show great challenges for the safety-critic tasks, so it is crucial to study the robustness of CV systems against physical attacks and the corresponding defense strategies.

General speaking, digital attacks and physical attacks are conducted on different stages within the visual recognition pipeline. For example, Fig.1 shows the difference between physical attacks and digital attacks via the traffic sign recognition task in self-driving scenario. We can see that for the physical attack, adversaries can implement attacks by manipulating the real-world stop sign or interfering the imaging of cameras. For the digital attack, adversaries usually directly generate adversarial perturbations on the pixels within the captured image or video by camera. No matter which kind of attacks, when the generated adversarial examples are input to the DNN models, they will lead to the wrong predictions. Compared to digital attacks, several crucial challenges of physical attacks are as follows:

(1) The physical adversarial example should resist the effect of camera imaging, which is mainly influenced by the optical lens and image sensor processor.

(2) The physical adversarial example need to retain robustness to different transformations, such as shooting distance changes, angle changes, and illustration changes.

(3) The physical adversarial example should be stealthy. Digital images are modified in pixel-level, which is hard to perceived. However, it is challenging for physical attacks to realize inconspicuousness.

To address the above issues, many works have been proposed to evaluate the physically adversarial robustness of DNNs in the past years. It is necessary to explore the current existing physical attack and defense methods, and

• Xingxing Wei, Bangzheng Pu and Jiefan Lu are with the Institute of Artificial Intelligence, Beihang University, No.37, Xueyuan Road, Haidian District, Beijing, 100191, P.R. China. Baoyuan Wu is with The Chinese University of HongKong, Shenzhen, P.R.China.
• Xingxing Wei is the corresponding author (E-mail: xxwei@buaa.edu.cn)

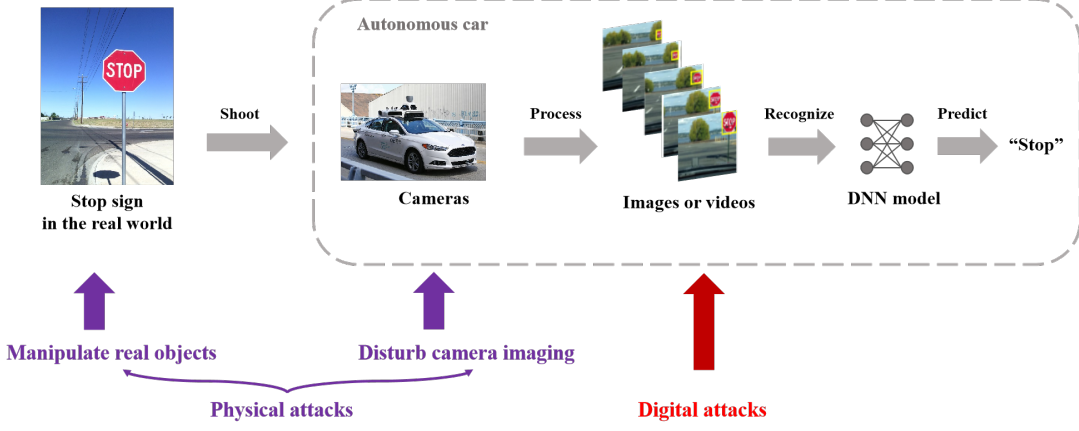


Fig. 1. The comparison between digital attacks and physical attacks in the standard visual recognition pipeline. Here we choose the traffic sign recognition as the example to show their differences.

TABLE 1

Published surveys of adversarial attacks and defenses in the computer vision task. The number of referred papers about physical attacks and defenses are counted in the last column.

Surveys	Physical attacks	Physical defenses	Year	Number
Chakraborty et al.[17]	✗	✗	2018	0
Akhtar et al.[2]	✓	✗	2018	8
Qiu et al.[103]	✓	✗	2019	8
Huang et al.[63]	✓	✗	2020	1
Akhtar et al.[3]	✓	✗	2021	34
Wei et al.[131]	✓	✗	2022	46
Ours	✓	✓	2022	90

give a summary for the current progress and future direction. Although there exist several surveys about adversarial attacks and defenses in computer vision, they are not comprehensive and latest versus physical attacks and defenses. For example, [17] concludes digital attacks and defenses that focus on different machine learning models, but not involves physical attacks and defense. Akhtar et al. [2] review adversarial attacks and defenses in computer vision before 2018, only some early-staged methods of physical attack are contained in the part of "Attacks in the real world". Later, Qiu et al. [103] introduce physical adversarial attacks as an application scenario of adversarial attacks in 2019. And then, in the years of 2020, Huang et al. [63] conclude studies in this filed in five parts: verification, testing, adversarial attacks and defences, and interpretability. After that, [3] systematically reviews adversarial attacks and defences, but the physical attacks are still not the key point. We can see that the above works mainly focus on introducing adversarial attacks and defenses in the digital domain, while leaving the physical parts alone. Recently, Wei et al. [131] publish a survey about the physical adversarial attacks in computer vision. They discuss the current physical attacks from effectiveness, stealthiness, and robustness, respectively. We are different from them versus three aspects: (1) Besides physically adversarial attacks, we also give a survey of the physically adversarial defenses, while [131] does not involve this topic. (2) We introduce and illustrate the current

physically adversarial attacks with a more refined classification from multi-level viewpoints (see Fig. 2), which is more systematic than [131]. (3) We discuss more referred papers of physical attacks and defenses than [131] (90 vs 46). A comparison is listed in Table 1 for these surveys. In brief, a comprehensive review for the latest physical attacks and defenses in computer vision is imperative.

For that, in this paper, we write a survey to systematically record the recent researches in this field for the last ten years. Specifically, we first establish a taxonomy of the current physical attacks from attack tasks, attack forms, and attack methods, respectively. For attack tasks, we introduce five safety-critical tasks where researchers usually conduct physical attacks. For attack forms, we conclude three main manners which the current physical attacks involve. For attack methods, we summary four attack settings from the white-box and black-box perspective. Secondly, we establish a taxonomy of the current physical defenses from three stages of a DNN model: pre-processing, in-processing, and post-processing. Each stage contains multiple fine-gained classification for the defense methods. Finally, we discuss seven existing challenges that are still unsolved in this field, and further outlook the future direction. The framework of this survey is illustrated in Fig. 2.

In summary, this survey has three main contributions:

(1) We establish a taxonomy of the current physical attacks from three perspectives: attack tasks, attack forms, and attack methods. We believe these three aspects can give a clear description for readers.

(2) We establish a taxonomy of the current physical defenses from three perspectives: pre-processing, in-processing, and post-processing for the DNN models to achieve a full coverage of the defense process.

(3) The physical attacks and defenses are still a rapidly developing research field, many problems need to be solved. So, we conclude challenges in this field and make a prospect towards the future direction.

The rest part of this paper is structured as follows: In section 2, we introduce the physically adversarial attacks. In section 3, we review the physically adversarial defenses. In section 4, we analysis challenges in this field and make an outlook of this research direction.

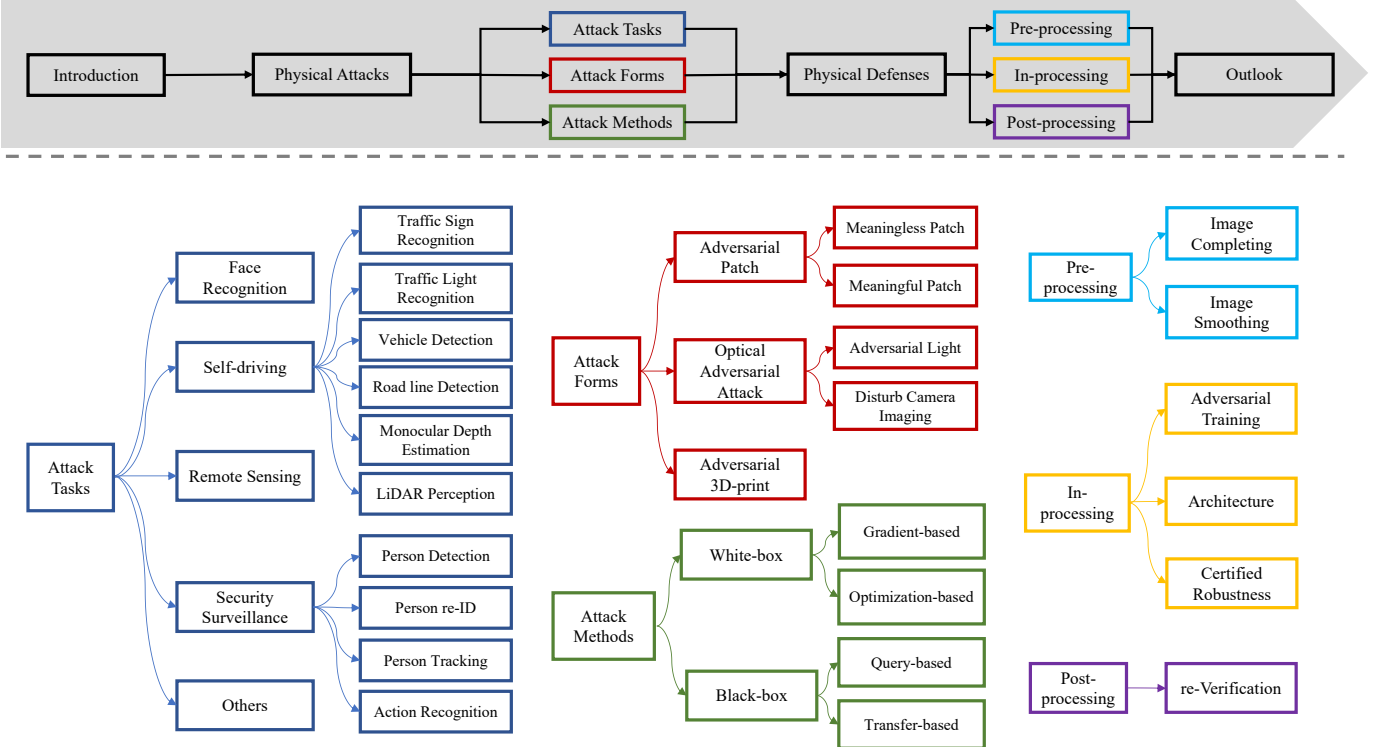


Fig. 2. The framework of this survey. We first establish the taxonomy of physically adversarial attacks and defenses, and then, the outlook for the future direction is discussed.

2 PHYSICALLY ADVERSARIAL ATTACKS

Physical attacks are carried out in the real world and become more threatening than digital attacks. Since Kurakin et al. [70] first demonstrate DNNs are vulnerable to physically adversarial examples, a lot of attention is poured to the physical domain. In this section, we introduce different attack tasks in physical scenarios, discuss physical forms of adversarial examples, and analyse attack methods in the white-box setting and the black-box setting (Representative methods in the different attack tasks are briefly exhibited in Table 2, 3, 4, respectively).

2.1 Attack tasks

Physical attacks are implemented in real-world scenarios that contain a wide variety of tasks. In these sections, we mainly introduce several safety-critical tasks, including face recognition, self-driving, security surveillance and remote sensing. Besides, we show the application of physical attacks against the embodied agent.

2.1.1 Face recognition

With the application of Face Recognition (FR) in mobile payments and identity verification, people are paying more and more attention to face security. Attackers can easily exploit wearable physically adversarial examples to masquerade as someone else, which will cause severe problems in privacy and property. Most researches divide attacks into dodging and impersonation. Like the untargeted attack, the goal of dodging attack is to misclassify a person's face into any other face. Attackers need to minimize the probability

of the original class. Like the targeted attack, impersonation attack aims to deceive a FR system to recognize a face as another specific face. To solve this problem, attackers minimize the distance between the model's output and the target class.

Early related approaches focus on white-box attacks. Sharif et al. [114] make adversarial glass frames, which can avoid being recognized by their local DNN face models or pretend to be another. To improve transferability, [68, 98] craft patches of different shapes to attack the public face model Arcface [32]. The adversarial patch in the physical environment requires strong anti-interference ability. Once the adversarial example fails, it is difficult for the attacker to update the pattern quickly. However, the adversarial light can be modified to adapt changes in physical environments. Zhou et al. [155] develop a non-contact face confrontation method. They fabricate a wearable hat with infrared LEDs to fool facial recognition systems. Recently, Nguyen et al. [95] propose to project digital patches on faces by off-the-shelf projectors, which does not require wearable devices.

Developing black-box methods is more valuable in the physical world than white-box methods. Some face recognition applications need to call commercial APIs, which can be accessed by attackers and obtain their outputs. Therefore, adversaries can pretend to be harmless users and produce adversarial examples by querying those APIs. Assuming that the target model is unknown, sharif et al. [114] update adversarial patterns by querying target models. Besides changing the perturbations, finding the vulnerable position is an important problem in the research of face patches. Attacking weak areas can not only improves efficiency but

TABLE 2
Representative physical attacks against face recognition systems

Task	Methods	Settings	Physical forms	Sources
Face recognition	Adv-Glass [114]	White&Black	Meaningless patch (Glassframe)	SIGSAC 2016
	AGNs [113]	Black	Meaningful patch (Glassframe)	TOPS 2019
	Pautov et al. [98]	White	Meaningless patch (Glassframe)	SIBIRCON 2019
	Adv-Hat [68]	White	Meaningless patch (Hat)	ICPR 2020
	Nguyen et al. [95]	White	Adversarial Light	CVPR 2020
	GenAP-DI [142]	Black	Meaningful patch (Makeup)	CVPR 2021
	Adv-Makeup [151]	Black	Meaningful patch (Makeup)	IJCAI 2021
	Guo et al. [133]	Black	Meaningless patch (Sticker)	Arxiv 2022
	Wei et al. [132]	Black	Meaningful patch (Sticker)	TPAMI 2022

also avoids overfitting. To search for the most vulnerable locations, Wei et al. [132] develop a query-based method to search for the cartoon sticker's adversarial locations and rotation angles. Compared to other methods, they do not need to calculate perturbations. However, a large number of queries in a short time may attract the attention of administrators. Guo et al. [133] propose to optimize location and perturbation simultaneously, which reduces the query numbers from thousands to a dozen times.

Most FR terminals can not be queried directly in our daily life, so adversaries must train adversarial examples in local models before transferring them to target models. Generative models are often used to fit the distribution of real data, which gives methods of generating adversarial examples with a good transferability. ANGs [113], Adv-Makeup [151], GenAP-DI [142] train a generator to produce imperceptible adversarial examples. They do not rely on accessibility but significantly improve the transferability in commercial models.



Fig. 3. Compared with AdvPatch [14] and RP2 [43], AdvCam [39] is more natural for the human vision. This figure comes from [39].

2.1.2 Self-driving

Ensuring people's life safety is a prerequisite for the application of autonomous driving technology. A self-driving system needs to deal with complex situations in the real world. It must keep the cars on the right road, avoid obstacles, pedestrians and other vehicles along the way, and accurately identify traffic signs, lights and lane lines. The physically adversarial attack can pose threats in all aspects, challenging the most important safety principle.

Traffic sign recognition In the early stage, attacks on traffic signs are usually carried out under the white-box setting. Lu et al. [85] propose an attack on traffic sign detection, but their method is not robust enough and needs to add large perturbations to be successful. Autonomous vehicles will take pictures of traffic sign recognition at different distances, angles, and weather conditions. In digital and physical domains, the expectation over transformation technique (EOT)

is introduced to improve the robustness. Shapeshifter [85] improves Attack Success Rate (ASR) with iterative attack and EOT. Unlike traditional EOT [5] technique performing the data augmentation in the preprocessing stage, RP2 [43] requires adversaries to shoot traffic signs in different settings as model inputs, which is more realistic than making transformations in the digital domain. Later, Eykholt et al. [118] expand RP2 from the classification to detection. Although those methods improve robustness, their adversarial patterns are still too noticeable. NatureAE [145] exploits an adaptive mask to limit perturbations in the pixel level, their method will try to reduce the perturbed pixel while maintaining the ASR as much as possible. AdvCam [39] (Fig.3) uses neural style transfer to create natural corrosion style stop signs, which can hide from human attention as well as keep large perturbations. Sitawarin et al. [117] propose a method to hide adversarial examples on billboards near traffic signs. They implement targeted attacks on billboard images to mislead the model's output as a traffic sign. Recently, Zhong et al. [154] propose to construct adversarial shadows by querying the target model, which is invisible and efficient (reach more than 90% ASR on LASA-CNN and GTSRB-CNN). IAP [7] generates inconspicuous patches in a progressive way, the visually invisible effect is evaluated using saliency maps and anonymous voting.

Traffic light recognition Traffic light recognition systems for autonomous vehicles require fine-tuning when they adapt to new cities. Patel et al. [97] propose a physical poisoning attack in the fine-tuning progress. They place a screen that plays a specific pattern based on the colour of the traffic light so that the DNN will learn the wrong correlation information, resulting in false predictions. This method is difficult to do physics experiments, so they implement it in a virtual engine instead. Recently, Zolfi et al. [158] make translucent stickers that cause the camera's optical lens to have a local out-of-focus effect and carried out a targeted attack on Tesla autopilot. Compared to [97], their methods are easier to implement and less likely to be discovered.

Vehicle detection For self-driving cars, immediately and correctly detecting surrounding vehicles is one of the crucial demands for safety. Adversarial patterns can cause great hazards by hiding vehicles from the CV perception. Due to safety and cost limitation, most relative researches [152, 138, 122, 128] conduct experiments on the virtual environment or by using toy cars [122, 128].

UPC [62] (Universal perturbation camouflage) is a general white-box attack framework against object detection,

TABLE 3
Representative physical attacks against autonomous driving systems

Sub-tasks	Methods	Settings	Physical Forms	Sources
Traffic sign recognition	Lu et al. [85]	White	Meaningless patch	ArXiv 2017
	RP2 [43]	White	Meaningless patch	CVPR 2018
	RP2D [118]	White	Meaningless patch	USENIX WOOT 2018
	Sitawarin et al. [117]	White	Meaningless patch	ArXiv 2018
	DT-UAPs [8]	White	Meaningless patch	ACCV 2020
	AdvCam [39]	White	Meaningful patch	CVPR 2020
	IAP [7]	Black	Meaningless patch	IOJT 2021
	SLAP [83]	White	Adversarial light	USENIX Security 2021
Traffic light recognition	Shadow attack [154]	Black	Meaningful patch	CVPR 2022
	Zolfi et al. [158]	Black	Disturb camera imaging	CVPR 2021
Vehicle detection	B&S [97]	White	Meaningful patch (Advertising board)	NeurIPS 2020 workshop
	CAMOU [152]	Black	Meaningless patch(Camouflage)	ICLR 2019
	ER [138]	Black	Meaningless patch(Camouflage)	ArXiv 2020
	UPC [62]	White	Meaningless patch	CVPR 2020
	DAS [128]	White	Meaningful patch	CVPR 2021
Road line detection	Abdelfattah et al. [1]	White	Meaningless patch(Camouflage)	CVPR 2022
	Boloor et al. [11]	Black	Meaningful patch (Adversarial line)	JSA 2020
Monocular Depth Estimation	Sato et al. [111]	White	Meaningful patch	USENIX Security 2021
	Yamanaka et al. [146]	White	Meaningless patch	IEEE Access 2020
LiDAR perception	Cheng et al. [24]	White	Meaningful patch	ECCV 2022
	Sun et al. [121]	Black	Adversarial Light (Spoofing Laser)	USENIX Security 2020
	Tu et al. [125]	White & Black	Adversarial 3D-print	CVPR 2020
	Abdelfattah et al. [1]	White	Adversarial 3D-print	ICIP 2020

its region proposal network (RPN), classification and regression network are simultaneously attacked, which makes it transferable on single-stage and two-stage detectors. Inspired by the interpretability of machine learning, Wang et al. [128] propose a Dual Attention Suppression (DAS) attack, which can cold the DNN heat map while diverting people's attention. However, the renderer used in DAS has a limited representation of physical properties. To gain more realistic renderings, Suryanto et al. [122] design a differentiable transformation network (DTN) to train an adversarial camouflaged patch.

CAMOU [152] and ER [138] both follow the black-box settings to implement query-based attacks. Zhang et al. [152] design an approximate gradient network to render adversarial camouflage with the unreal-4 engine, which provides a convenient way to set the camera's parameters. To alleviate the cost of computation, Wu et al. [138] use a discrete searching algorithm and enlarge-and-replicated technique to produce the camouflage from a small patch.

Road line detection Lane line detection is an important technique for ensuring that the car does not deviate from the right road lane. Boloor et al. [11] propose a query-based method that produces adversarial black lines to attack an autonomous simulator.

Automated Lane Centering (ALC) is a level-2 self-driving technique that helps autonomous cars to keep their centre on the street. It is widely used in mainstream commercial models such as Tesla AutoPilot, NioPilo, and SuperCruise. Early Tencent [71] paints fake road lines to fool Tesla Autopilot, but it does not implement a drive-by test on the road with a lane line. Sato et al. [111] propose to produce a dirty road patch to deceive ALC systems. Their method is evaluated on OpenPilot and achieves 97.5% ASR in 80 attack scenes. The mean successful time is 1.6 seconds lower than

the average driver reaction time.

Monocular Depth Estimation Monocular Depth Estimation (MDE) is a critical auxiliary of the fully vision-based ADS, which can expand perception from 2D to 3D space. Yamanaka et al. [146] first attack MDE with adversarial patches in white-box settings. Their purpose is to optimize the depth values in the patch region to certain depth values, and [49] is used to generate conspicuous perturbations iteratively. Besides, they adopt some common transformation techniques to improve patches' robustness. Real world experiments show the poor transferability between two MDE models [72, 52]. To balance stealthiness and effectiveness, Cheng et al. [24] propose a natural-style patch whose size is controlled by a differentiable mask. They evaluated transferability on three MDE models and demonstrated the impact on downstream 3D reconstruction tasks.

LiDAR perception Except for visual autopilot, some modern autonomous driving systems (ADS) rely on LiDAR perception. LiDAR point clouds will not be perturbed by image-level adversarial examples, so it is more difficult to attack LiDAR-based ADS. So far, there are two mainstream physical attacks against LiDAR perception systems. One is to construct a three-dimensional adversarial mesh [125, 1], the other is to launch an adversarial laser to interfere with the normal LiDAR scanning process [121, 78].

Tu et al. [125] produce the adversarial 3D mesh both in white-box and black-box settings. They first render the mesh into a point cloud, then use the approximate roof technique to make the point cloud fit the vehicle's rooftop and modify the mesh vertices to minimize the confidence score of the target vehicle. Abdelfattah et al. [1] design a multimodal framework to generate 2D images and 3D point clouds simultaneously by rendering a 3D mesh. To generate an adversarial 2D image, the attacker deforms the 3D mesh

by adding a vector to each vertex, assigning RGB values to the vertices and interpolating to shade the faces. The mesh is placed on the car's roof and projected as a 2D image. To get the point cloud, the Moller-Trumbore cross-section algorithm [91] is used to compute the intersections between the laser beam and mesh triangles in space. However, the 3D adversarial mesh is difficult to manufacture precisely and will inevitably discard some adversarial features when sampled as point clouds.

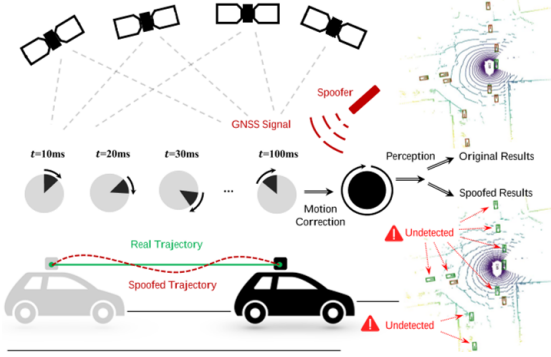


Fig. 4. The process of trajectory attack. Green/red denotes the ground truth/prediction. This figure comes from [78].

Recently, some research [15, 99, 115, 121, 78] show that the LiDAR perception system (LPS) is vulnerable to harmful lasers. Sun et al. [121] propose the first black-box spoofing attack against LPS. They manipulate lasers to simulate occlusion patterns and sparse point clouds far from autonomous cars. By thinking about the mechanisms of GNSS and trajectory compensation, Li et al. [78] propose a trajectory attack (Fig.4), which produces the adversarial signal to spoof the motion correction.

In conclusion, launching adversarial laser is more suitable for attacking LiDAR perception, but mesh has the advantage of implementing multimodal attacks against both LiDAR and visual systems.

2.1.3 Security surveillance

In order to improve social security, intelligent security monitoring is widely used in scenarios such as crime tracking and illegal behaviour identification. Physical adversarial examples can be used by criminals to evade security surveillance, which will cause potential security threats.

Person detection Person detection is a basic task for security surveillance, such as flow monitoring and criminal tracking. Adversarial attacks against person detection systems might be exploited to avoid security checks by the crime. Pedestrian detection can be mainly divided into methods based on visible light images and infrared image recognition used to compensate for nighttime and poor lighting conditions.

In visible-light person detection, Thys [123] et al. are the first to use a white-box attack against the single-stage detector (YOLOv2 [106]), where they print the adversarial pattern onto a piece of cardboard and hold it in hand to evade pedestrian detection. To control environmental variables in physical experiments, Huang [62] et al. create a standard evaluation dataset named *AttackScene* in the virtual environment. Most researchers also investigate the

transferability to verify their cross-model ability [140, 144, 60, 61, 156, 157], which is evaluated on mainstream single-stage (YOLO series [107, 106]...) and two-stage detectors (Faster-RCNN [108]). To make adversarial examples robust to clothing deformations, Wu et al. [140] and Xu et al. [144] consider the deformation of the non-rigid body before generating patches on clothes. They project adversarial patterns with Thin Plate Spline (TPS) [119] mapping. Recently, Hu et al. [61] propose TC-EGA (Toroidal-Cropping-based Expandable Generative Attack) to generate an adversarial texture with repetitive patterns, which can adapt to different viewpoints of the camera. To produce natural adversarial patterns, Hu et al. [60] train a BigGAN[13] to control specific category generation.

In infrared person detection, Zhu et al. [156] craft a bulb board to interfere with infrared person detection. They indirectly adjust the two-dimensional Gaussian distribution of the light source by optimizing the parameters of the small bulb array, which can greatly reduce the computational cost compared to the pixel-level calculation. Recently, Zhu et al. [157] manufacture infrared invisibility clothes (Fig. 5), which are made of thermal insulation material (TIM) and ordinary fabric. Under thermal camera imaging, the region covered by TIM is dark, and the rest is bright. Therefore, adversaries can exploit this to generate a black and white adversarial pattern, which looks like the "QR code".

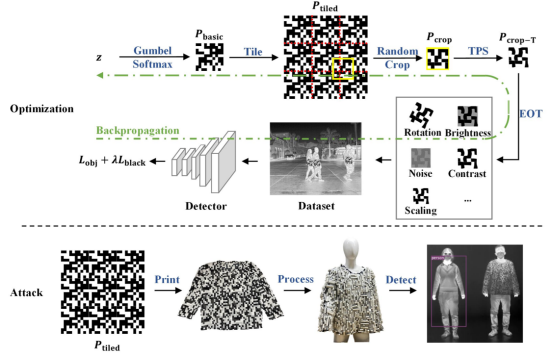


Fig. 5. Generating the adversarial "QR code" pattern and making infrared invisibility clothes. This figure comes from [157].

Person re-ID Person re-identification (re-ID) can be used in security surveillance, it is a sub-problem of image retrieval, aiming to match a person of interest in different camera views. Due to different shooting views and distance, changes in dress, and environmental conditions, attacking re-ID models has become a challenging problem. Wang et al. [130] propose the first physical attack against re-ID models. They implement evading attacks for identification mismatch and impersonation attacks for target person impersonation. In the physical experiment, they make adversarial clothes and choose different shooting angles and distances. The result shows 60% matching precision drop under evading attack and 67.9% mAP of impersonation attack.

Person tracking Unlike person detection, person tracking requires quick responses to the moving person, and it is usually modelled as a similarity matching problem [9, 74]. Previous attacks of single object tracking are mostly implemented in the digital domain [22, 147, 139], which are not transferred well in physical settings. Wiyatno and Xu [135]

TABLE 4
Representative physical attacks against security surveillance systems

Sub-tasks	Methods	Settings	Physical Forms	Sources
Person detection	Huang et al. [62]	White	Meaningless patch (Clothes)	CVPR 2020
	Wu et al. [140]	Black	Meaningless patch (Clothes)	ECCV 2020
	Xu et al. [144]	Black	Meaningless patch (T-shirt)	ECCV 2020
	Hu et al. [60]	Black	Meaningful patch (Clothes)	ICCV 2021
	Zhu et al. [156]	Black	Adversarial Light	AAAI 2021
	Hu et al. [61]	Black	Meaningless patch (Clothes)	CVPR 2022
	Zhu et al. [157]	Black	Meaningless patch (Infrared invisibility clothes)	CVPR 2022
Person re-ID	Wang et al. [130]	White	Meaningless patch (Clothes)	ICCV 2019
Person tracking	PAT [135]	White	Meaningless patch (Poster)	ICCV 2019
	Ding et al. [33]	White	Meaningless patch (Clothes)	AAAI 2021
Action recognition	Pony et al. [102]	White	Adversarial light	CVPR 2021

propose a method of generating the adversarial texture, which is exhibited on a screen or poster. However, it requires a large area of perturbations that cover the background, which is impractical for attacking trackers outdoors. Due to spatial texture stationary in raw image [46, 70], Ding et al. [33] propose Maximum Textural Discrepancy (MTD), which is used to maximise the discrepancy between the template image and the search image. In the physical attack, they conduct experiment on state-of-art trackers (SiamRPN++ [75], SiamMask [129]) and achieve over 40% ASR.

Action Recognition The action recognition model takes a time-series image as input. Thus the attacker needs to update adversarial examples in each frame, but physical adversarial examples are difficult to change immediately, such as adversarial patches. Pony et al. [102] propose an implementable approach to mislead action recognition by controlling the LED light. Instead of computing the perturbation for each pixel, they add an RGB offset with the same value for each frame.

2.1.4 Remote sensing

Remote sensing is closely related to public safety and national security. The remote sensing image is shot by drones or satellites, and the image quality is challenged by the atmospheric condition and the distance between the camera and objects. Czaja et al. [29] attack the aerial image classifier and mention the potential influence of the atmosphere. Hollander et al. [59] attempt to camouflage large-sized military assets such as aircraft and warships. However, they do not carry out the physical attack in the real world. Du et al. [37] first implement physical attacks on aerial images, and they generate patches not only on the top of vehicles but also on off-and-around cars. Besides, they consider the effects of weather and season, but the ablation study show that compounding disparate weather does not improve the ASR.

2.1.5 Others

Embodied agent With the development of multi-modal techniques and virtual environments, the embodied agent is used to simulate real interactions with humans and their surroundings. The embodied question and answering (EQA) [30, 31] and embodied vision recognition (EVR) [148] are utilized to realize speech and visual interactions. Liu et

al. [79] propose a novel spatiotemporal attack for embodied agent. The agent finds the chessboard from different rooms to answer the question. At the same time, the attacker generates perturbations in the target 3D object of deceiving the agent (These local perturbations can be crafted as patches in the physical world). Results show that their method causes dramatically accuracy drop for question answering (40% to 5% on average) and visual recognition (89.91% to 18.32%).

2.2 Attack forms

Before a physical attack is implemented, the adversarial example needs to be manufactured appropriately. Attackers often focus on whether a method is feasible in a real environment, including how to resist adverse environmental effects, facilitate manufacture, and prevent the adversarial pattern from being detected by the human eye. This section introduces attack forms mainly from adversarial patches, optical adversarial attacks, and 3D printed adversarial objects.

2.2.1 Adversarial patches

The adversarial patch is the most popular approach in the physical attack. Digital attacks generate perturbation in the whole image, which is impractical for implementing adversarial attacks in the real world, while patches only modify local pixels. It can be printed easily and can be pasted on the target directly. A mask is generally used to control the shape of the perturbed area. After the adversarial patch is optimized in the digital domain, the adversarial patch will be crafted and placed on the surface of the object. The adversarial patch can be defined as:

$$I_{adv} = M \odot I(x + \delta) + (\mathbf{1} - M) \odot I, \quad (1)$$

where I is the clean object, and $I(x + \delta)$ denotes the adversarial perturbations. M is the mask, $M_{i,j} \in \{0, 1\}^d$, where $\mathbf{1}$ is a unit matrix which has the same size as M . Adversarial patches can be divided into meaningless patches and meaningful patches according to the pattern in $I(x + \delta)$ (Fig.6).

(1) Meaningless patches

From the perspective of human observation, meaningless patches do not correspond to objects in the real world. In order to generate a meaningless patch, attackers need to calculate the perturbed values of each pixel. For the white-box attack, patterns on the patch are usually optimized by

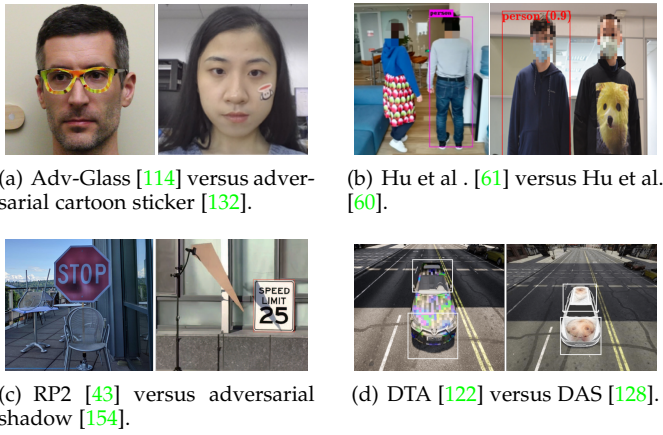


Fig. 6. Visual difference between meaningless patches (Left) and meaningful patches (Right).

gradient-based methods, like iterative FGSM [68, 98, 95] etc. and C&W [43, 118, 117, 19, 149] etc. In black-box settings, particle swarm optimization (PSO) [114], Reinforcement learning (RL) [133] etc. are used for optimization.

To make adversarial patches look smoother, attackers minimize the TV loss [120] to reduce the variations between adjacent pixels. The TV loss can be expressed as follows:

$$\mathcal{L}_{TV} = \sum_{i,j} \sqrt{(x'_{i,j} - x_{i+1,j})^2 + (x'_{i,j} - x_{i,j+1})^2}, \quad (2)$$

where the (i,j) is the pixel of the coordinate. Digital adversarial examples can display rich colours. For a real-world attack, printer colours are limited. Sharif et al. [114] first propose a non-printed score (NPS) to eliminate printed colour error, which can be declined by:

$$\mathcal{L}_{nps} = \sum_{\hat{p} \in \hat{P}} \prod_{p \in P} |\hat{p} - p|, \quad (3)$$

where $P \subset [0, 1]^3$ is the set of printable RGB space, \hat{P} is the set of the pixel value in adversarial pattern, \hat{p} represents one pixel's RGB value of the adversarial pattern, p is the printable colour and $p \in P$. [68, 98] follow Adv-Glass's [114] settings and add TV loss to the objective function. In Adv-Hat [68], NPS does not make influence on their experiments. Pautov et al. [98] change the RGB image to grey level, which cleverly avoids adding NPS loss. Nguyen et al. [95] change RGB to LAB space to eliminate the aberration of the projection pattern.

Adversarial patches are pasted on the surface of 3D objects, such as human faces, cars, and clothes. These curved surfaces might destroy the effectiveness of the adversarial pattern, so it is necessary for attackers to model deformations. For the human face, Pautov et al. [98] train a grid generator to simulate Non-linear transformation, and then they project the adversarial pattern on the grid. Komkov et al. [68] use STL (spatial transformation layer) to project the perturbation on a hat. STL includes two steps: off-plane bending and pitch rotation. In order to realize wearable adversarial examples, Wu et al. [140] and Xu et al. [144] model non-rigid deformations by TPS [119]. [144] shows that modeling the deformation can significantly improve

ASR from 48%-74% against YOLOv2, and 34%-61% against Faster-RCNN [108]. Hu et al. [61] introduce the Toroidal Cropping (TC) technique, which can project points from a two-dimensional plane onto a torus by two folds. The best texture is searched by random cropping at the junction of the recurring patch plane.

(2) Meaningful patches

The patch that humans can recognize as a real object is meaningful. Most existing meaningful patches [113, 60, 142, 151] are generated by GAN. Adversaries generally train a generator to produce realistic or natural-style adversarial patches [145, 39, 24].

Face stickers are common every day and can be seen at festivals or large events. Recently, Wei et al. [132] optimize cartoon stickers' location and rotation angle to achieve a high success rate against the face recognition system. They do not need to compute each pixel value of adversarial patterns. Thus their method is easier to implement and more threatening.

Inspired by natural shadows, Zhong et al. [154] produce adversarial shadows in the real world and achieve a 95% success rate. They construct a triangular area and use the PSO strategy to search for the optimal location by optimizing three coordinates of vertices. In order to adjust the brightness of shadows, they manipulate the L channel of LAB space according to SBU Shadow dataset [126], they statistic the mean ratio of pixel values of LAB triple channels to simulate settings of realistic shadows.

However, DAS [128] combines the meaningful patch and meaningless patch. As shown in Fig.6 (b), the patch generated by DAS consists of two parts: the outline of a smiling face and the texture of illegible patterns. Neural networks prefer texture information when extracting features, so the adversarial texture is used to deceive the attention of DNN. At the same time, a meaningful contour is used to distract human attention, which makes the adversarial texture inconspicuous.

2.2.2 Optical adversarial attack

CV systems must have optical perception modules, which leave a "loophole" for physically adversarial attacks. Adversaries can use the imaging principle of the camera and the characteristics of the image sensor processor to attack. Based on existing research, we divide Optical Adversarial Attacks into adversarial lights and disturb camera imaging.

(1) Adversarial lights

A simple approach to expand adversarial patches from printable picture to visible-light is achieved by light projection. Nguyen et al. [95] propose a feasibly real-time physical attack on the FRS by projecting light on human faces. They first calibrate settings of the camera and projector on attacked scenes, then generate the adversarial pattern in digital world and project it on the face to deceive FRS. There are two critical calibration steps (position and color calibration) to ensure effectiveness of the attack. Besides, they analyse some reasons caused failure cases, such as intensive ambient-light, terrible facial poses and projector out of focus. Lovisotto et al. [83] craft Short-Lived Adversarial Perturbations (SLAP) with projecting RGB light on the stop sign. To adapt illumination changes, They do frame interpolation by synthesizing static images, which give sensors



Fig. 7. The framework of adversarial light projection. Due to the background lighting, The table shows only project the adversarial illumination with environment loss compensation can successfully fool the VGG-16. This figure is from [47].

time to response thus eliminate subtle noise of camera in non-bright conditions. SLAP shows a high ASR on SentiNet [26], which is a state-of-art defense method against adversarial patches. Gnanasambandam et al. [47] implements an adversarial attack through an artificially designed lighting distribution. Instead of adding the perturbation to the image, they model the image transformation from a projector to a camera, optimizing the structured lights' parameters by gradient methods. The process is shown in Fig.7.

To achieve imperceptibility, Sayles et al. [112] exploit the rolling shutter effect (RSE) in commercial cameras to create stripe patterns on objects, which both can deceive classifiers and be invisible to human eyes. They adopt a differentiable representation of RSE to compute perturbed patterns by the end-to-end gradient-based method. In practice, a RGB LED produces modulated illumination at a frequency higher than human perception. Laser Pointers, such as teaching tools or pets' toys, are commonly used in our daily life. Duan et al. [40] propose a method to optimize the parameters of laser and use a laser pointer to implement attacks easily.

Zhou et al. [155] exploit consumer infrared LED to produce adversarial light spots on the face. Firstly, they compute the spotlight's optimal parameters (position, brightness and size). Secondly, they launch hardware on the brim of a baseball cap to facilitate illuminating the face stealthily. Zhu et al. [156] manufacture a matrix of bulbs to fool the thermal infrared pedestrian detectors. The bulb is chosen to be the light source due to its brightness well reflect thermal properties. The temperature and pixel of a single bulb approximately follow a Gaussian distribution. If putting many bulbs on cardboard satisfies the 2D Gaussian distribution. The parameters that need to be optimized are thousands of times less than pixel-level patches.

(2) Disturb camera imaging

The camera lens and image sensor processor (ISP) play important roles in the final image quality, so they can be used as a backdoor to implement the physical attack. Disturb camera imaging specifically exploit the principles of optical imaging rather than disrupt the functions and structure of hardware.

According to the image-forming principle, ISP transforms the row image into the RGB image. Phan et al. [100] develop a method that deceives the camera ISP. They design an approximate neural network for the ISP and compute perturbations by solving a multi-task optimized problem. Attacking a specific camera can be realized by adding constrained terms in the objective function. Due to consumer



Fig. 8. Translucent patches are stuck to the camera lens and successfully hide the stop sign under the detector. This figure comes from [158].

cameras adopting several mainstream ISPs, and different ISPs containing some same pipelines like demosaicing, their method is effective for ISP transferred attacks against other black-box optical imaging systems.

Li et al. [77] place a well-designed translucent sticker (TS) on the camera lens against classifiers. Due to the patterns on translucent stickers being out of focus, a small opaque dot put on the camera lens will create a blurred translucent pattern in the final image. They model this effect and synthesis adversarial perturbations in the digital domain. However, in practice, most parameterizations can not be realized in the physical world. Alternatively, they use structural similarity (SSIM) to measure the similarity between the clean image and the dot image. In detail, firstly, a linear transformation is fitted by 50 printed colours for mapping from the actual RGB to the digital RGB. The greedy searching algorithm finds optimal locations and colours that achieve the highest loss. Finally, fine-tuning locations by gradient descent. In the real-world attack, ten dots-TS achieved nearly 50% ASR against ResNet-50. Later, Zolfi et al. [158] expand camera stickers to attack detectors. As shown in Fig.8, the model fails to detect the stop sign but correctly recognizes other objects. In the real-wold autonomous, they attack the ADAS's (Advanced Driving Assistance System) perception on Tesla model X, successfully fooling the system into identifying red lights as green.

2.2.3 Adversarial 3D-print

Although physical attacks on 2D images have exposed severe security problems, little research has been reported on 3D perception. For the 3D adversarial attack, the coordinate changes to a triplet (x, y, z) , which increases optimiza-

tion's complexity and challenges crafting physical forms. A framework of adversarial 3D-print is shown in Fig.9. Tsai et al. [124] put forward a novel approach to creating printable adversarial objects in the physical world. They print 3D objects after producing adversarial examples in the digital domain, but attacks mostly fail for complex objects during re-sampling, which can drop the information of perturbed point clouds. Wen et al. [134] propose Geometry-Aware Adversarial Attack (*GeoA*³) and craft 3D printed adversarial objects. In order to better preserve adversarial effects when re-sampling point clouds from the surface meshes, *GeoA*³-IterNormPro is used to optimize perturbations via iterative normal projection. Compare to [124] in physical attacks, [134] show a better result in different models.

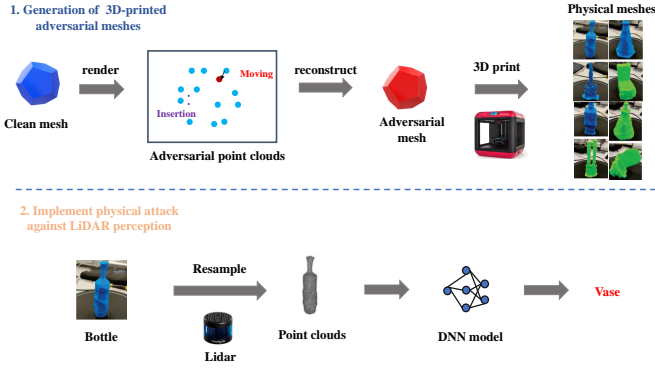


Fig. 9. 3D-printed adversarial attack including two steps: (1) Generation of 3D-printed adversarial meshes. Firstly, a clean mesh is rendered to point clouds. Secondly, add an offset to a point or insert new points and optimize parameters to achieve an attack in the digital domain. Thirdly, reconstruct point clouds to adversarial meshes. Finally, print 3D objects according to adversarial meshes; (2) Implement physical attack against LiDAR perception. 3D-printed objects will be resampled by LiDAR sensors, which may drop some adversarial point clouds. This figure is from [124].

2.3 Attack methods

According to the existing research's main purpose and settings, we divide the attack methods into white-box and black-box attacks. In the real world, it is difficult to gather the knowledge of the target model, so the black-box attack is more practical.

2.3.1 White-box attacks

We introduce the white-box attacks in the physical attacks from gradient-based methods and optimization-based method, respectively.

(1) Gradient-based attacks

Most white-box attacks generate perturbations based on the gradient information of the target model. Goodfellow et al. [70] improve FGSM and propose a basic iterative method (BIM) used in the first physical attack. Furthermore, they suggest using the label of the least-likely class to implement the targeted attack. Wiyatno et al. [135] generate the physical adversarial texture (like colourful art) by FGSM, which controls the gradient direction. The Projected Gradient Descent (PGD) [86] is another widely used powerful method that projects the gradient to a ball. Madry et al. [86] prove the PGD is the L_∞ bounded I-FGSM. Later, improvements of

I-FGSM appeared, Momentum iterative [35] is used against local optimum, and applying image transformations [143] for enhancing input diversity.

In most physical cases, parameters can be optimized directly with gradient descent in the white-box setting. Singh et al. [116] propose to generate robust adversarial examples against light changes by exploiting nonlinear brightness transformation and PGD attack. However, sometimes attackers must establish differentiable models themselves so that the gradient propagates in the framework of producing adversarial examples [47, 122, 100, 112]. The gradient-based method can achieve a high success rate in white-box settings, but their performances usually drop when transferred to other black-box models.

(2) Optimization-based attacks

Some works show that gradient-based methods are non-effective on models with defence mechanisms, such as adversarial training [86] and knowledge distillation [96]. In such a case, the optimization-based attacks are available.

Carlini & Wagner [16] regard solving the adversarial example as a box-constrained optimization problem:

$$\min D(x, x + \delta) + c \cdot f(x + \delta), \quad s.t. \quad x + \delta \in [0, 1]^n, \quad (4)$$

they construct a series of objective functions $f(\cdot)$ for better optimization and simplify the original non-linear constrain, $D(\cdot)$ is the distance, which bounded the perturbation with L_0 , L_∞ and L_2 , c is a hyperparameter that balance terms. Results show that C&W attack can break the KD defense, even some other defensive methods.

Due to its good performance, many attack methods follow the C&W-like objective function. To fool the traffic sign classified model, Eykholt et al. [43] add EOT and NPS on basic C&W. Yang et al. [149] use C&W attack against outputs of the SSD model with constrains of colours and brightness, the objective function calculates the logits distance between the original class and the target class. Pony et al. [102] propose the modified C&W loss function. Considering the quadratic loss term smoothing the gradients and momentum of the optimizer, they define the loss function as non-negative and take the minimum between the linear item and the quadratic term as the value of the loss function. In order to achieve imperceptibility, two regularization terms are introduced to constrain the first and second-order temporal derivatives: the first controls temporal changes of the perturbation, and the second penalizes rapid trend changes. Tsai et al. [124] generate adversarial point clouds and real print objects. They adopt the basic C&W loss function with a small modification. Unlike the image, the perturbation of point clouds is represented by a vector, which includes the direction and the magnitude of shift points. The Chamfer distance [44] is used as an alternative way to measure the distance between the original point and the shifted point. Although the C&W attack is effective against various visual task models, the adversarial example still lacks the transferability and inconspicuousness.

2.3.2 Black-box attacks

In the physical world, adversaries can only access the limited information about target models. Therefore, it is more valuable to study attack methods under black-box

settings. In this part, we divide black-box attacks into query-based and transfer-based attacks.

(1) Query-based attacks

For the query-based attack, we assume that the training data and the target model are unknown but allow the attacker to obtain the output of the target model, such as probability or class.

Evolution algorithm Wei et al. [132] propose a printed-irrelevant attacked method by manipulating the position and rotation angle of the adversarial sticker (Fig.6(a)). As those parameters are discrete variations, they adapt the evolution strategy instead of gradient-based methods to search for optimal resolutions. The traditional evolutionary algorithm [127] generates the offspring by crossover and mutation between the random individuals in parents, this promise the diversity of parents while leading to a slow rate of convergence. Inspired by the positional aggregation phenomenon of successfully attacked patches, parameters of the sticker are efficiently solved by Region based Heuristic Differential Evolutionary Algorithm (RHDE), which finds the offspring near the superior solution of each parent generation. The criterion of the offspring selection (unfitness) adapts the value of the objective function. Their method is easy to implement in the physical environment, and thanks to PAP, there is no need to place stickers precisely.

Reinforcement learning Inspired by behaviourist psychology, Reinforcement Learning (RL) focuses on how agents take action in an environment to maximize certain cumulative rewards. Guo et al. [133] design a RL framework to simultaneously optimize positions and perturbation values of the adversarial patch in black-box settings. However, directly optimizing perturbations and positions will lead to many queries. Thus they propose to adjust the attacked step size and the weight of each surrogate model to shrink the parameter space. To further improve the transferability and reduce the number of queries, they exploit the RL framework to adjust parameters. Compared with RHDE [132] (only change the position) and ZO-AdaMM [20] (only change the perturbation), [133] decreases the number of queries tens or hundreds of times less. Results show that they achieve a high ASR in some popular face recognition models (FaceNet, ArcFace34 and CosFace50) and a few decline in commercial API, but it is enough to threaten FR models in the real world.

Particle swarm optimization(PSO) PSO is a heuristic algorithm to find optimal solutions by simulating the foraging behaviour of the flock. Sharif et al. [114] use PSO to compute adversarial examples to implement impersonation attacks by querying Face++. Due to Face++ only returning the top three classes (candidates), the optimization process will be hard to continue when the target is not in these classes. Thus they propose a recursive impersonation algorithm to fix this problem.

Compared to other black-box methods, Sharif et al. [114] believe PSO is more efficient in computation than the genetic algorithm, and it is more resource efficient than training surrogate models. The zero-order optimization (ZOO) [18] is a popular approach to estimating gradients of the target model. However, Zhong et al. [154] find that the gradient explodes and vanishes when they use ZOO to optimize their discrete variables (coordinates of shadows in [154]) and

Boolean value. Alternatively, they exploit the PSO strategy. Their goal is to deceive traffic sign recognition models by producing adversarial shadows on real-world signs. The terminal condition is that the class of adversarial example is not equal to the original class or the iteration number reaches maximum.

Greedy strategy Duan et al. [40] generate adversarial laser beam(AdvLB) by manipulating a laser pointer in the physical world. The laser beam is defined by four parameters including wavelength, layout(angle and intercept), width and intensity, which are optimized by greedy strategy with random-restarts in each iteration. In order to make AdvLB realizable, attackers can adapt parameters in an effective range which is calculated by a batch of transformed images.

(2) Transfer-based attacks

For transfer-based attacks, we assume that the target model is unknown, but all or part of the training data can be obtained. Adversaries train a substitute model to generate adversarial examples and implement attacks against the target model based on the transferability of the adversarial example.

Ensemble attacks Ensemble training has been widely used to improve the generalization and robustness of DNN models. Similarly, the idea can be expanded to adversarial attacks. [140, 144, 60, 156] adopt ensemble attack to improve transferability, which achieved balanced results on different models. Zhu et al. [156] take the sum of detector loss as the ensemble loss. Wu et al. [140] propose an ensemble loss to help their method transfer to detectors that are not used in training:

$$\min \mathbb{E}_T \sum_{i,j} \max\{f^j(x_i') + 1, 0\}^2, \quad (5)$$

where \mathbb{E}_T represents EOT, and $f^j(x_i')$ means the prediction of i -th object in j -th detector. Xu et al. [144] introduce the min-max optimization to physically ensemble attack:

$$\min \max \mathbb{E}_T \sum_j^M \sum_i^N w_i f^j(x_i') - \alpha \|w - 1/N\|_2^2 + \lambda g(\delta), \quad (6)$$

where α and λ are regularization parameters, and w are domain weights that help balance detectors' importance. When $\alpha = 0$, the ensemble loss gets the maximum. when $\alpha \leftarrow \inf$, $w \leftarrow 1/N$, the ensemble loss is the average.

Generative adversarial examples Generative Adversarial Network (GAN) [48] provides a framework to train a neural network for producing data close to real distribution. It generally consists of a generator $\mathcal{G}(\cdot)$ and a discriminator $\mathcal{D}(\cdot)$. In our settings, $\mathcal{G}(\cdot)$ is used to generate adversarial examples by inputting $\mathcal{D}(\cdot)$, and $\mathcal{D}(\cdot)$ is a local DNN model, which is used to measure the difference between generate images and clean images. During the training process, parameters of \mathcal{G} and \mathcal{D} are updated iteratively and alternately. The generator can significantly improve the diversity of adversarial examples with less training data and produce realistic images for human eyes.

Sharif et al. [113] first propose a framework of GAN for generating adversarial patches. In order to deceive the FR system, they collect pictures of glass frames from Google and pre-train a generator to produce different colours and textures with a fixed mask. They successfully implement

the impersonation attack on open source models and black-box platforms (Aliyun, Face++) in the digital world. In the physical experiment, they attack FaceNet, CosFace, and ArcFace. Kong et al. [69] design PhysGAN for producing imperceptible adversarial posters at the roadside board. In order to maintain the robustness of adversarial examples in the physical world, videos shot by a camera in the car are used to pre-train the target model. In the physical experiment, they attack several popular CNN-based steering models (NVIDIA Dave-2, Udacity Cg23, Udacity Ramb) and evaluate the physically adversarial effectiveness against NVIDIA Dave-2 on a real car. Jan et al. [66] exploit conditional GAN to simulate the digital to physical (D2P) process. After GAN generates the D2P transformation, EOT is used to generate adversarial examples. The D2P simulator is conducive to producing many D2P-style images, but it adds noise to the whole image. In the real world, adversaries only select the specific object in the foreground to add perturbations. In Bai et al. [7], the vulnerable location of the image is guided by the attention map. They adopt a coarse-to-fine way to generate perturbations. In the generative process, the perturbation produced by the generator at the upper level is prior to the lower level. Their method shows good transferability and successfully implements attacks on five kinds of traffic signs in the real world.

Meta attacks Meta-learning can obtain a good initialization parameter of a model by designing a series of training tasks. Thus it can improve the performance of the model on new tasks. In adversarial attacks, meta-learning can be used to enhance the transferability of generative adversarial examples. In D2P process, the printed distortion and shape transformations will decrease the effectiveness of the physically adversarial example. Feng et al. [45] propose a class-agnostic and model-agnostic meta-learning (CML) algorithm to train a robust generative model, which can simulate D2P transformed adversarial examples. The CML includes two stages: 1) meta-training for the generative model; 2) fine-tuning for unknown attack tasks. Therefore, the CML can realize the few-shot learning and significantly improve adversarial examples' generalization ability. Yin et al. [151] also adopt meta-learning to train an adversarial make-up generator, producing natural and transferable eye make-up. In the meta-training process, assuming that there are n target models, firstly, they choose $n-1$ models that share the same generator to implement the attack. Secondly, the remaining model as a meta-test model, and repeat the above procedure until all models are tested. In the physical experiments, they achieve the best ASR compared to adv-Hat [68] and adv-Glass [114] in two popular commercial FR systems (Face++ and Microsoft).

3 PHYSICALLY ADVERSARIAL DEFENSES

In this section, we review the literature in computer vision for physically adversarial defenses. To help readers achieve a comprehensive understanding of the physically adversarial defenses, we organize the methods from three stages for the DNN models, i.e., pre-processing, in-processing, and post-processing. The taxonomy is given in Fig.10. Specifically, in section 3.1, we discuss the mechanism

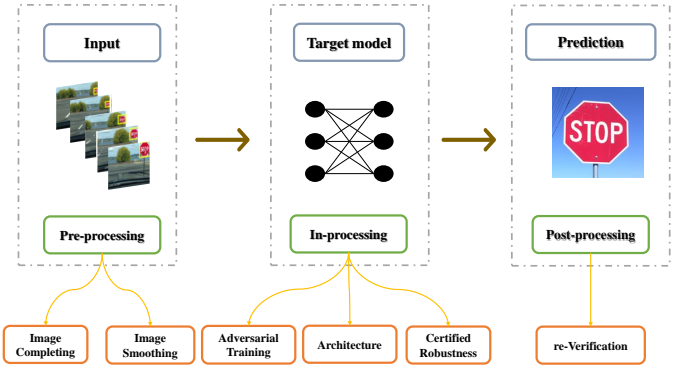


Fig. 10. A framework for adversarial defense methods against physical adversarial attacks in different processing stages.

of pre-processing defenses. In Section 3.2, we divide the in-processing defense methods into adversarial training, architecture modification and certified defenses, respectively. In section 3.3, the post-processing methods are discussed. In addition, Table 5 lists a summary for the referred physically adversarial defenses. From the table, we can see that the existing physically adversarial defenses are mainly proposed against adversarial patches. This is reasonable because adversarial patches are currently the main form of physically adversarial attacks.

3.1 Pre-processing

Data pre-processing can reduce the impact of physical perturbations. The current pre-processing methods can be divided into image completing and image smoothing. .

3.1.1 Image completing

Image completing defenses [41, 51, 80] first localize the patch regions through the differences between adversarial patches and their neighboured regions. And then, defenders can complete these regions based on the localized regions. In this way, the effects of adversarial attacks are removed.

Digital watermarking (DW) [56] uses the magnitude of the saliency maps to detect abnormal regions and then masks them out from the input. SentiNet [26] utilizes Gradient-weighted Class Activation Mapping (Grad-CAM) to obtain the mask. In order to mask the patch area more efficiently, the SAC [80], and MR [87] algorithms utilize the segmentation technique. Firstly, the patch segmenter predicts the initial irregular patch region, which will be complemented by the shape completer [80] or 3×3 region voting [87]. Secondly, the mask covered the whole patch region is recovered to turn the wrong prediction to correct one. Recently, TaintRadar [76] finds a strong correlation between adversarial regions and the rank of classes. It uses negative masks against patch attacks by alternating three forward-propagations and two back-propagations. The change in the rank of Top-K logits observed in the forward propagation can guide the generation of the negative mask during the back-propagation. K logits correspond to the K negative masks.

TABLE 5
Representative physical defense methods mentioned in this paper

Categories	Methods	Modes	Attack Forms	Sources
Pre-processing	DW [56]	Empirical Defense	Adversarial Patch	CVPR 2018
	LGS [94]	Empirical Defense	Adversarial Patch	WACV 2019
	SentiNet [26]	Empirical Defense	Adversarial patch	SPW 2020
	MR [87]	Empirical Defense	Adversarial patch	ACNS 2020
	BlurNet [104]	Empirical Defense	Adversarial patch	DSN-W 2020
	TaintRadar [76]	Empirical Defense	Adversarial patch	INFOCOM 2021
	SAC [80]	Empirical Defense	Adversarial Patch	CVPR 2022
In-processing	ROA [137]	Empirical Defense	Adversarial patch	Arxiv 2019
	AT-LO [105]	Empirical Defense	Adversarial patch	ECCV 2020
	IBP for patch [25]	Certifiable Defense	Adversarial Patch	ICLR 2020
	Clipped BagNet [153]	Certifiable Defense	Adversarial Patch	SPW 2020
	(De)Randomized Smoothing [73]	Certifiable Defense	Adversarial Patch	NeurIPS 2020
	Ad-YOLO [67]	Empirical Defense	Adversarial Patch	Arxiv 2021
	MAT [88]	Empirical Defense	Adversarial patch	ICML 2021
	RSA [93]	Certifiable Defense	Adversarial Patch	ICML 2021
	PatchGuard [141]	Certifiable Defense	Adversarial Patch	ICLR 2021
	PatchVote [64]	Certifiable Defense	Adversarial Patch	Arxiv 2021
	BAGCERT [89]	Certifiable Defense	Adversarial Patch	ICLR 2021
	ScaleCert [54]	Certifiable Defense	Adversarial Patch	NeurIPS 2021
	MultiBN [82]	Certifiable Defense	Adversarial Patch	TIP 2021
	DeRS-ViT(chen) [23]	Empirical Defense	Adversarial Patch	CVPR 2022
	DeRS-ViT(salman) [110]	Certifiable Defense	Adversarial Patch	CVPR 2022
	Demasked Smoothing [150]	Certifiable Defense	Adversarial Patch	Arxiv 2022
Post-processing	KEMLP [53]	Empirical Defense	Adversarial patch	ICML2021
	DDDM [21]	Empirical Defense	Adversarial patch	Arxiv2022

3.1.2 Image smoothing

Randomized Smoothing [28] adds Gaussian noises with different magnitudes to an adversarial example. All the noisy adversarial examples are then classified through a base classifier, and the voting of these classifications is reported as the result. (De)Randomized Smoothing [73] uses the fixed-width image ablation to generate smoothed images (illustrated in Fig.11). In this way, the number of the smoothed images affected by the adversarial patch can be calculated. This quantitative framework is beneficial for the improvement of model robustness. The ViT model also adopts this framework to defend patch attacks [23, 110]. Local Gradients Smoothing (LGS) [94] directly smooths the patch regions. It splits the picture into 5x5 patches and applies slide-windows to look for the highest activation regions. Then, it smooths these regions to eliminate adversarial patches. Previous image smoothing strategies can not guarantee the integrity of the image. Therefore, they are not suitable for image segmentation tasks. Demasked Smoothing [150] reconstructs the ablative image with ZITS [34]. In this way, the segmentation model can achieve the same predictions on adversarial examples as clean images.

In addition, in the frequency domain of the image, [104] finds adversarial attacks usually introduce the high-frequency noises. So it proposes a BlurNet model, which introduces low-pass filtering into the feature maps of the network's first layer. The low-pass filtering can remove the high-frequency noise to defend the RP2 attack.

3.2 In-processing

Pre-processing defense is usually time-consuming. Therefore, it is necessary to improve the robustness of the DNN model itself. The existing methods are mainly from

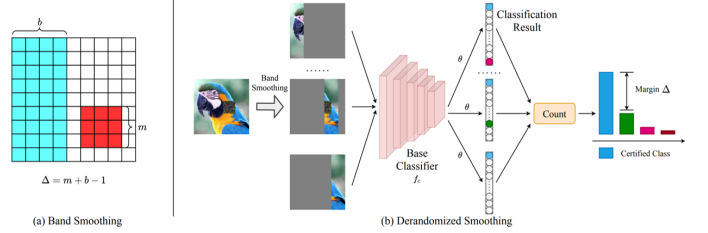


Fig. 11. Introduction of the (De)Randomized Smoothing. On the left, the patch's width is m , and the width of the column ablation is b . Specifically, let Δ be the number of smoothed images affected by adversarial patches. On the right, the smoothed images are fed into the base classifier to vote for the final result. This figure comes from [23].

three perspectives: adversarial training, architecture modification, and certified robustness.

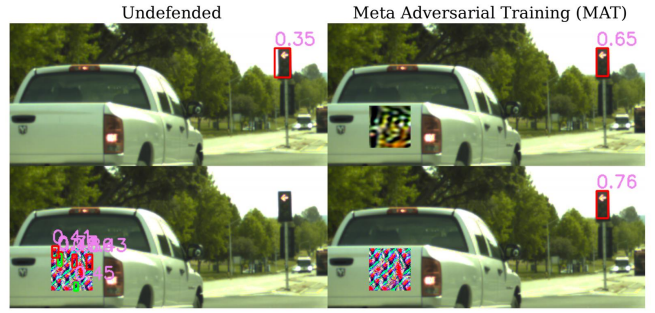


Fig. 12. Illustration of MAT model trained on the Bosch Small Traffic Light datasets. This figure comes from [88].

3.2.1 Adversarial training

Adversarial training (AT) uses adversarial examples as training data to improve the robustness of the model. [86, 49, 16]. The goal of AT is recovering the clean prediction for adversarial examples, which can be optimized by:

$$\min_{\theta} \mathbb{E}_{(x,y) \sim \mathcal{D}} \left[\max_{\Delta x \in \Omega} L(x + \Delta x, y; \theta) \right]. \quad (7)$$

Researchers use physically adversarial examples to train the target DNN models. Wu et al. [137] exploit AT to defend the rectangular occlusion attacks (ROA), which are used to attack traffic signs. Rao et al. [105] finds that just using fixed locations of adversarial patches is insufficient against location-optimized adversarial patches. Therefore, full location optimization (four directions) and random location optimization (random direction) are adopted to optimize the patch location. The model trained on a single category patch is deficient [57]. Therefore, the content of the patches needs to be optimized. Meta-adversarial training (MAT) [88] combines adversarial training with meta-learning to improve the generalization of the adversarial training model. It uses different meta-patches with different step sizes to generate adversarial examples in an original image. As shown in Fig.12, MAT can obtain the correct prediction for different adversarial examples.

3.2.2 Architecture modification

Researchers can modify the network's architecture to weaken the effect of adversarial patches on the final classification. Existing methods are mainly from two aspects: 1) Narrowing the receptive field. 2) Introducing new neural units.

1) Narrowing receptive fields is inspired by BagNet [12], which adopts the structure of ResNet-50. BagNet reduces the receptive field size by replacing the 3×3 convolution kernels with 1×1 convolution kernel. Moreover, BagNet extracts features from each small image patch to generate per-patch logits and calculate the average. Therefore, adversarial patches can only exist in a few regions when attacking BagNet. Clipped BagNet [153] and PatchGuard [141] both use BagNet as the backbone network. To further ensure the robustness of the model, Clipped BagNet artificially abandons the abnormal logits before averaging them, and PatchGuard adopts a robust masking aggregation to detect and mask the abnormal feature.

The self-attention mechanism of ViT also limits the "receptive field". Adversarial patches can only affect a portion of the tokens. PatchVote [64] uses a 16×16 patch size ViT model [36] to perform voting on different patches' predictions.

2) Introducing new neural units can efficiently solve the optimization problem of the model when its architecture is changed. Ad-YOLO [67] adds the "Patch" class in the last layer of a YOLO-v2 while keeping other layers unchanged. In this way, Ad-YOLO can simultaneously identify adversarial patches and recover correct predictions. MultiBN [82] introduces a dynamic batch normalization (BN) layer structure against multiple types of adversarial videos (including physically adversarial videos) for video recognition. For a specific adversarial video, a learnable BN layer module selects its corresponding BN layer, which provides more

precise distribution estimations. This BN layer selection mechanism is beneficial to improve the generalization of the defense model. Han et al. propose a robust model ScaleCert [54] based on superficial important neurons (neurons susceptible to disturbances). ScaleCert masks them during inference to eliminate the effects of patches. To improve the robustness of ViT, RSA [93] adopts a robust aggregation (RAG) mechanism, which scores all tokens and discards outliers to weaken the effect of patch attacks. Metzen et al. propose the BAGCERT defense [89] to classify images by a region scorer (3-layer CNN with kernel sizes 3, 1, and 3) and a spatial aggregator.

3.2.3 Certified robustness

The above empirical defenses lack theoretical guarantee for their robustness. To solve this problem, researchers propose certified defenses and prove that their models are robust under different circumstances. The model has certified robustness when the input and output (x, y) satisfy the following:

$$\underline{m}_y = \mathcal{Z}_{y_{true}}^{(K)} - \overline{\mathcal{Z}}_y^{(K)} \geq 0 \quad \forall y. \quad (8)$$

In this discriminant, \underline{m}_y is the certified distance boundary in [136]. $\mathcal{Z}_y^{(K)}$ denotes the output of layer k . This means that the lower bound of the output of the true class is always greater than (at least equal to) the upper bound of any other output y .

The first certified defense is based on Interval Boundary Propagation (IBP) [50], which is commonly used in digital defense. Later, Chiang et al. [25] expand IBP to defend adversarial patches. The model outputs a differentiable lower bound (verifiable radius), which is the distance between true labels and other labels. Therefore, the model can be trained to increase the distance. The following equation can calculate the boundary distance:

$$(e_{y_{true}} e_y)^T \mathcal{Z}^{(K)} = \underline{m}_y \geq 0 \quad \forall \mathcal{Z}^{(0)} \in \mathbb{B}(x_0) \quad \forall y. \quad (9)$$

Here, e_i is the i^{th} basis vector, $\mathbb{B}(x_0)$ is the set of constraints on the possible range of the adversarial input image.

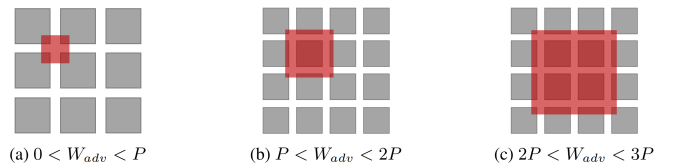


Fig. 13. The number of ViT patches affected by adversarial patches with different sizes. This figure comes from [64].

Cohen et al. [28] use Randomized Smoothing to ensure the certified robustness of the model in digital attacks. To apply Randomized Smoothing in patch defenses, Levine et al. [73] propose (De)randomized smoothing and do smoothing outside the partial region. Theoretically, model robustness is certified when a quantitative boundary's maximum exceeds the second-largest classification result:

$$n_c(X) > \max_{\substack{c' \\ c' \neq c}} n_{c'}(X) + 2\Delta. \quad (10)$$

In extreme cases, all the Δ images are misclassified to wrong class but the number of smoothed images with true class

is still the largest. Recently, Demasked Smoothing [150] combines image Smoothing with Region Reconstruction to maintain the integrity of inputs in the segmentation.

BagNet is an important model in the field of certified defense. Clipped BagNet [153] proves that certified robustness can be achieved as long as enough abnormal blocks are clipped before the feature aggregation stage. PatchGuard [141] evaluates all possible mask predictions. If all predictions are consistent, the final prediction will be certified robust. BAGCERT [89] couples model training and robustness verification by an end-to-end region scorer and spatial aggregator. Region scorer gives linear region scores for the true and non-true classes of the image. Then the spatial aggregator calculates the difference between these two scores, which can be used for robustness certification and training.

With the development of the ViT [36], certified defenses have started using ViT as the base classifier. PatchVote [64] utilizes a pre-trained ViT-B/16 as backbone model. PatchVeto produces certified predictions on input images by manipulating ViT's self-attention and voting on different tokens' predictions. The validation result is produced by voting on all tokens' predictions:

$$v(x) \triangleq \begin{cases} 1, & \text{if } f_1(x) = f_2(x) = \dots = f_k(x) = f(x) \\ 0, & \text{otherwise} \end{cases} \quad (11)$$

As shown in Fig.13, at least one patch can completely cover the adversarial patch. The predictions are validated if all Transformer encoders agree on the same class of predictions. Salman et al. [110] and Chen et al. [23] respectively combine the ViT model with (De)randomized smoothing. Their methods both replace the original ViT's global self-attention (SA) with isolated band unit SA. Therefore, the speed of the inference is greatly accelerated.

3.3 Post-processing

The mechanism of post-processing defenses is consistent with the thinking process of humans [42]: re-Verification, which inspires researchers to conduct post-processing. After making a preliminary prediction, models must comprehensively analyze more evidence.

Gürel et al. [53] combine domain knowledge and adversarial defense in Knowledge Enhanced Machine Learning pipeline (KEMLP), which builds factor graphs by modeling ML models' outputs and the KEMLP predictions, and different factors have different logical relationships with the target. Taking the "Stop" street sign as an example, the word "Stop" is a sufficient condition, and "Octagon" is a necessary condition. The logical judgment of each factor will integrate domain knowledge to form the final output. This re-Verification process can effectively avoid illogical misclassification, such as "Stop" to "speed limit".

Inspired by the Drift-Diffusion Model (DDM) [109] and Dropout method [58], Chen et al. [21] propose the Dropout-based Drift-Diffusion Model (DDDM). Firstly, they apply dropout to produce clipped models of the target model. Secondly, the output of every clipped model is used to do a threshold accumulation. The final robust output is produced when the decision evidence accumulates to a certain threshold.

4 OUTLOOK

The physically adversarial attacks and defenses have been developed rapidly in recent years, especially for the adversarial patch, which has been deployed in different target models and scenarios in the real world and shown actual threats. However, many intractable problems are still worth to be discussed. In this section, we analysis these challenges and predict research directions of physically adversarial attacks and defenses in the future.

(1) Transferable Physically Adversarial Attacks

For real-world attack applications such as face recognition, autonomous driving, and security monitoring, white-box attacks are difficult to implement, and commercial systems do not support querying. Therefore, only transfer-based attacks can be utilized. However, the current transfer-based adversarial attacks in the physical environment are still relatively weak. It is worthy of an in-depth study.

(2) Robust Physically Adversarial Attacks

Physically adversarial examples must maintain effectiveness in different shooting angles, distances and lighting conditions and adapt to the camera's various processing. How to remain the effectiveness in these changing circumstances is a challenge, and is worthy of an in-depth study.

(3) Stealthy Physically Adversarial Attacks

Physical attacks tend to produce conspicuous perturbations for sensing devices to capture adversarial patterns effectively, which brings a big problem in realising stealthiness. Constructing device-perceptible while human-imperceptible physical attacks is a challenge, and is worthy of an in-depth study.

(4) Natural Physically Adversarial Attacks

Existing works concentrate on constructing artificially adversarial examples. However, there are many naturally formed adversarial examples in real life, such as images captured in the clouds, rain, fog or captured at a specific viewpoint. These phenomena have threat to the autonomous driving system. Thus, how to find these adversarial examples is challenging.

(5) Universal Physically Adversarial Defenses

Existing physical defenses are primarily designed against adversarial patches, but various forms of attacks also exist. It is impossible to design the specific defense method for each attack form, so finding a mechanism to construct an universal physical defence is necessary.

(6) Efficient Physically Adversarial Defenses

No matter pre-processing, adversarial training or post-processing defense methods, all of them bring additional computation, so it is challenging to design an efficient defense without extra computation cost. For example, designing the new network's architecture.

(7) Trade-off Physically Adversarial Defenses

Similar to digital defenses, physical defenses will also face the trade-off problem between accuracy and robustness. According to characteristics of the physical attack, it is challenging to eliminate this trade-off, and is worthy of an in-depth study.

REFERENCES

- [1] Mazen Abdelfattah et al. "Towards universal physical attacks on cascaded camera-lidar 3d object detection models". In: *ICIP*. IEEE. 2021, pp. 3592–3596.

[2] Naveed Akhtar and Ajmal Mian. "Threat of adversarial attacks on deep learning in computer vision: A survey". In: *Ieee Access* 6 (2018), pp. 14410–14430.

[3] Naveed Akhtar et al. "Advances in adversarial attacks and defenses in computer vision: A survey". In: *IEEE Access* 9 (2021), pp. 155161–155196.

[4] Mohd Ansari, Dushyant Kumar Singh, et al. "Human detection techniques for real time surveillance: A comprehensive survey". In: *MTA* 80.6 (2021), pp. 8759–8808.

[5] Anish Athalye et al. "Synthesizing robust adversarial examples". In: *ICML*. PMLR. 2018, pp. 284–293.

[6] Claudine Badue et al. "Self-driving cars: A survey". In: *ESWA* 165 (2021), p. 113816.

[7] Tao Bai, Jinqi Luo, and Jun Zhao. "Inconspicuous Adversarial Patches for Fooling Image Recognition Systems on Mobile Devices". In: *IOT* (2021).

[8] Philipp Benz et al. "Double targeted universal adversarial perturbations". In: *ACCV*. 2020.

[9] Luca Bertinetto et al. "Fully-convolutional siamese networks for object tracking". In: *ECCV*. 2016, pp. 850–865.

[10] Sweta Bhattacharya et al. "Deep learning and medical image processing for coronavirus (COVID-19) pandemic: A survey". In: *SCS* 65 (2021), p. 102589.

[11] Adith Boloor et al. "Attacking vision-based perception in end-to-end autonomous driving models". In: *JSA* 110 (2020), p. 101766.

[12] Wieland Brendel and Matthias Bethge. "Approximating cnns with bag-of-local-features models works surprisingly well on imagenet". In: *arXiv preprint:1904.00760* (2019).

[13] Andrew Brock, Jeff Donahue, and Karen Simonyan. "Large scale GAN training for high fidelity natural image synthesis". In: *arXiv:1809.11096* (2018).

[14] Tom B Brown et al. "Adversarial patch". In: *arXiv preprint:1712.09665* (2017).

[15] Yulong Cao et al. "Adversarial sensor attack on lidar-based perception in autonomous driving". In: *ACM SIGSAC*. 2019, pp. 2267–2281.

[16] Nicholas Carlini and David Wagner. "Towards evaluating the robustness of neural networks". In: *2017 iee sp*. 2017, pp. 39–57.

[17] Anirban Chakraborty et al. "Adversarial attacks and defences: A survey". In: *arXiv preprint:1810.00069* (2018).

[18] Pin-Yu Chen et al. "Zoo: Zeroth order optimization based black-box attacks to deep neural networks without training substitute models". In: *AI Sec*. 2017, pp. 15–26.

[19] Shang-Tse Chen et al. "Shapeshifter: Robust physical adversarial attack on faster r-cnn object detector". In: *ECML-PKDD*. Springer. 2018, pp. 52–68.

[20] Xiangyi Chen et al. "Zo-adamm: Zeroth-order adaptive momentum method for black-box optimization". In: *NeurIPS* 32 (2019).

[21] Xiyuan Chen et al. "DDDM: a Brain-Inspired Framework for Robust Classification". In: *arXiv preprint:2205.10117* (2022).

[22] Xuesong Chen et al. "One-shot adversarial attacks on visual tracking with dual attention". In: *CVPR*. 2020, pp. 10176–10185.

[23] Zhaoyu Chen et al. "Towards Practical Certifiable Patch Defense with Vision Transformer". In: *CVPR*. 2022, pp. 15148–15158.

[24] Zhiyuan Cheng et al. "Physical attack on monocular depth estimation with optimal adversarial patches". In: *arXiv preprint arXiv:2207.04718* (2022).

[25] Ping-Yeh Chiang et al. "Certified defenses for adversarial patches". In: *arXiv preprint:2003.06693* (2020).

[26] Edward Chou, Florian Tramer, and Giancarlo Pellegrino. "Sentinel: Detecting localized universal attacks against deep learning systems". In: *SPW*. IEEE. 2020, pp. 48–54.

[27] Gioele Ciaparrone et al. "Deep learning in video multi-object tracking: A survey". In: *Neurocomputing* 381 (2020), pp. 61–88.

[28] Jeremy Cohen, Elan Rosenfeld, and Zico Kolter. "Certified adversarial robustness via randomized smoothing". In: *ICML*. PMLR. 2019, pp. 1310–1320.

[29] Wojciech Czaja et al. "Adversarial examples in remote sensing". In: *ACM SIGSPATIAL*. 2018, pp. 408–411.

[30] Abhishek Das et al. "Embodied question answering". In: *CVPR*. 2018, pp. 1–10.

[31] Abhishek Das et al. "Neural modular control for embodied question answering". In: *CoRL*. PMLR. 2018, pp. 53–62.

[32] Jiankang Deng et al. "Arcface: Additive angular margin loss for deep face recognition". In: *CVPR*. 2019, pp. 4690–4699.

[33] Li Ding et al. "Towards Universal Physical Attacks on Single Object Tracking". In: *AAAI*. Vol. 35. 2. 2021, pp. 1236–1245.

[34] Qiaole Dong, Chenjie Cao, and Yanwei Fu. "Incremental transformer structure enhanced image inpainting with masking positional encoding". In: *CVPR*. 2022, pp. 11358–11368.

[35] Yinpeng Dong et al. "Boosting adversarial attacks with momentum". In: *CVPR*. 2018, pp. 9185–9193.

[36] Alexey Dosovitskiy et al. "An image is worth 16x16 words: Transformers for image recognition at scale". In: *arXiv:2010.11929* (2020).

[37] Andrew Du et al. "Physical adversarial attacks on an aerial imagery object detector". In: *WACV*. 2022, pp. 1796–1806.

[38] Meiyan Du. "Mobile payment recognition technology based on face detection algorithm". In: *CCPE* 30.22 (2018), e4655.

[39] Ranjie Duan et al. "Adversarial camouflage: Hiding physical-world attacks with natural styles". In: *CVPR*. 2020, pp. 1000–1008.

[40] Ranjie Duan et al. "Adversarial laser beam: Effective physical-world attack to DNNs in a blink". In: *CVPR*. 2021, pp. 16062–16071.

[41] Gintare Karolina Dziugaite, Zoubin Ghahramani, and Daniel M Roy. "A study of the effect of jpg compression on adversarial images". In: *arXiv preprint:1608.00853* (2016).

[42] Gamaleldin Elsayed et al. "Adversarial examples that fool both computer vision and time-limited humans". In: *NeurIPS* 31 (2018).

[43] Ivan Evtimov et al. "Robust physical-world attacks on machine learning models". In: *arXiv preprint* :1707.08945 2.3 (2017), p. 4.

[44] Haoqiang Fan, Hao Su, and Leonidas J Guibas. "A point set generation network for 3d object reconstruction from a single image". In: *CVPR*. 2017, pp. 605–613.

[45] Weiwei Feng et al. "Meta-Attack: Class-agnostic and Model-agnostic Physical Adversarial Attack". In: *ICCV*. 2021, pp. 7787–7796.

[46] Leon A Gatys, Alexander S Ecker, and Matthias Bethge. "Image style transfer using convolutional neural networks". In: *CVPR*. 2016, pp. 2414–2423.

[47] Abhiram Gnanasambandam, Alex M Sherman, and Stanley H Chan. "Optical adversarial attack". In: *ICCV*. 2021, pp. 92–101.

[48] Ian Goodfellow et al. "Generative adversarial nets". In: *NeurIPS* 27 (2014).

[49] Ian J Goodfellow, Jonathon Shlens, and Christian Szegedy. "Explaining and harnessing adversarial examples". In: *arXiv:1412.6572* (2014).

[50] Sven Gowal et al. "Scalable verified training for provably robust image classification". In: *ICCV*. 2019, pp. 4842–4851.

[51] Chuan Guo et al. "Countering adversarial images using input transformations". In: *arXiv preprint:1711.00117* (2017).

[52] Xiaoyang Guo et al. "Learning monocular depth by distilling cross-domain stereo networks". In: *ECCV*. 2018, pp. 484–500.

[53] Nezihe Merve Gürel et al. "Knowledge enhanced machine learning pipeline against diverse adversarial attacks". In: *ICML*. 2021, pp. 3976–3987.

[54] Husheng Han et al. "ScaleCert: Scalable Certified Defense against Adversarial Patches with Sparse Superficial Layers". In: *NeurIPS*. Vol. 34. 2021, pp. 28169–28181.

[55] Shijie Hao, Yuan Zhou, and Yanrong Guo. "A brief survey on semantic segmentation with deep learning". In: *Neurocomputing* 406 (2020), pp. 302–321.

[56] Jamie Hayes. "On visible adversarial perturbations & digital watermarking". In: *CVPR Workshops*. 2018, pp. 1597–1604.

[57] Jan Hendrik Metzen, Nicole Finnie, and Robin Hutmacher. "Meta Adversarial Training against Universal Patches". In: *arXiv e-prints* (2021).

[58] Geoffrey E Hinton et al. "Improving neural networks by preventing co-adaptation of feature detectors". In: *arXiv preprint:1207.0580* (2012).

[59] Richard den Hollander et al. "Adversarial patch camouflage against aerial detection". In: *AIMLDA II*. Vol. 11543. *SPIE*. 2020, 115430F.

[60] Yu-Chih-Tuan Hu et al. "Naturalistic Physical Adversarial Patch for Object Detectors". In: *ICCV*. 2021, pp. 7848–7857.

[61] Zhanhao Hu et al. "Adversarial Texture for Fooling Person Detectors in the Physical World". In: *arXiv:2203.03373* (2022).

[62] Lifeng Huang et al. "Universal physical camouflage attacks on object detectors". In: *CVPR*. 2020, pp. 720–729.

[63] Xiaowei Huang et al. "A survey of safety and trustworthiness of deep neural networks: Verification, testing, adversarial attack and defence, and interpretability". In: *Comput Sci Rev* 37 (2020), p. 100270.

[64] Yuheng Huang and Yuanchun Li. "Zero-Shot Certified Defense against Adversarial Patches with Vision Transformers". In: *arXiv e-prints* (2021).

[65] Andrew Ilyas et al. "Adversarial examples are not bugs, they are features". In: *NeurIPS* 32 (2019).

[66] Steve TK Jan et al. "Connecting the digital and physical world: Improving the robustness of adversarial attacks". In: *AAAI*. Vol. 33. 01. 2019, pp. 962–969.

[67] Nan Ji et al. "Adversarial yolo: Defense human detection patch attacks via detecting adversarial patches". In: *arXiv:2103.08860* (2021).

[68] Stepan Komkov and Aleksandr Petiushko. "Advhat: Real-world adversarial attack on arcface face id system". In: *ICPR*. IEEE. 2021, pp. 819–826.

[69] Zelun Kong et al. "Physgan: Generating physical-world-resilient adversarial examples for autonomous driving". In: *CVPR*. 2020, pp. 14254–14263.

[70] Alexey Kurakin, Ian Goodfellow, Samy Bengio, et al. *Adversarial examples in the physical world*. 2016.

[71] Tencent Keen Security Lab. *Experimental security research of Tesla autopilot*. 2019.

[72] Jin Han Lee et al. "From big to small: Multi-scale local planar guidance for monocular depth estimation". In: *arXiv preprint:1907.10326* (2019).

[73] Alexander Levine and Soheil Feizi. "(De) Randomized smoothing for certifiable defense against patch attacks". In: *NeurIPS* 33 (2020), pp. 6465–6475.

[74] Bo Li et al. "High performance visual tracking with siamese region proposal network". In: *CVPR*. 2018, pp. 8971–8980.

[75] Bo Li et al. "Siamrpn++: Evolution of siamese visual tracking with very deep networks". In: *CVPR*. 2019, pp. 4282–4291.

[76] Fengting Li et al. "Detecting localized adversarial examples: A generic approach using critical region analysis". In: *IEEE INFOCOM*. 2021, pp. 1–10.

[77] Juncheng Li, Frank Schmidt, and Zico Kolter. "Adversarial camera stickers: A physical camera-based attack on deep learning systems". In: *ICML*. 2019, pp. 3896–3904.

[78] Yiming Li et al. "Fooling lidar perception via adversarial trajectory perturbation". In: *ICCV*. 2021, pp. 7898–7907.

[79] Aishan Liu et al. "Spatiotemporal attacks for embodied agents". In: *ECCV*. 2020, pp. 122–138.

[80] Jiang Liu et al. "Segment and Complete: Defending Object Detectors against Adversarial Patch Attacks with Robust Patch Detection". In: *arXiv:2112.04532* (2021).

[81] Yanpei Liu et al. "Delving into transferable adversarial examples and black-box attacks". In: *arXiv:1611.02770* (2016).

[82] Shao-Yuan Lo and Vishal M Patel. "Defending against multiple and unforeseen adversarial videos". In: *IEEE TIP* 31 (2021), pp. 962–973.

[83] Giulio Lovisotto et al. "{SLAP}: Improving Physical Adversarial Examples with {Short-Lived} Adversarial Perturbations". In: *USENIX Security* 21. 2021, pp. 1865–1882.

[84] Dengsheng Lu and Qihao Weng. "A survey of image classification methods and techniques for improving classification performance". In: *IJRS* 28.5 (2007), pp. 823–870.

[85] Jiajun Lu, Hussein Sibai, and Evan Fabry. "Adversarial examples that fool detectors". In: *arXiv:1712.02494* (2017).

[86] Aleksander Madry et al. "Towards deep learning models resistant to adversarial attacks". In: *arXiv preprint:1706.06083* (2017).

[87] Michael McCoyd et al. "Minority reports defense: Defending against adversarial patches". In: *ACNS*. Springer. 2020, pp. 564–582.

[88] Jan Hendrik Metzen, Nicole Finnie, and Robin Hutmacher. "Meta adversarial training against universal patches". In: *arXiv preprint:2101.11453* (2021).

[89] Jan Hendrik Metzen and Maksym Yatsura. "Efficient certified defenses against patch attacks on image classifiers". In: *arXiv:2102.04154* (2021).

[90] Miss Sapana K Mishra, Faizpur Jtmcoe, KS Bhagat, et al. "A survey on human motion detection and surveillance". In: *IJARECE* 4 (2015).

[91] Tomas Möller and Ben Trumbore. "Fast, minimum storage ray-triangle intersection". In: *JGT* 2.1 (1997), pp. 21–28.

[92] Seyed-Mohsen Moosavi-Dezfooli, Alhussein Fawzi, and Pascal Frossard. "Deepfool: a simple and accurate method to fool deep neural networks". In: *CVPR*. 2016, pp. 2574–2582.

[93] Norman Mu and David Wagner. "Defending against adversarial patches with robust self-attention". In: *ICML Workshop*. 2021.

[94] Muzammal Naseer, Salman Khan, and Fatih Porikli. "Local gradients smoothing: Defense against localized adversarial attacks". In: *WACV*. IEEE. 2019, pp. 1300–1307.

[95] Dinh-Luan Nguyen et al. "Adversarial light projection attacks on face recognition systems: A feasibility study". In: *CVPR Workshops*. 2020, pp. 814–815.

[96] Nicolas Papernot et al. "Distillation as a defense to adversarial perturbations against deep neural networks". In: *IEEE SP*. 2016, pp. 582–597.

[97] Naman Patel et al. "Bait and switch: Online training data poisoning of autonomous driving systems". In: *arXiv preprint:2011.04065* (2020).

[98] Mikhail Pautov et al. "On adversarial patches: real-world attack on ArcFace-100 face recognition system". In: *SIBIRCON*. IEEE. 2019, pp. 0391–0396.

[99] Jonathan Petit et al. "Remote attacks on automated vehicles sensors: Experiments on camera and lidar". In: *Black Hat Europe* 11.2015 (2015), p. 995.

[100] Buu Phan, Fahim Mannan, and Felix Heide. "Adversarial imaging pipelines". In: *CVPR*. 2021, pp. 16051–16061.

[101] Athanasios S Polydoros and Lazaros Nalpantidis. "Survey of model-based reinforcement learning: Applications on robotics". In: *JINT* 86.2 (2017), pp. 153–173.

[102] Roi Pony, Itay Naeh, and Shie Mannor. "Over-the-air adversarial flickering attacks against video recognition networks". In: *CVPR*. 2021, pp. 515–524.

[103] Shilin Qiu et al. "Review of artificial intelligence adversarial attack and defense technologies". In: *Applied Sciences* 9.5 (2019), p. 909.

[104] Ravi S Raju and Mikko Lipasti. "Blurnet: Defense by filtering the feature maps". In: *2020 DSN-W*. IEEE. 2020, pp. 38–46.

[105] Sukrut Rao, David Stutz, and Bernt Schiele. "Adversarial training against location-optimized adversarial patches". In: *ECCV*. Springer. 2020, pp. 429–448.

[106] Joseph Redmon and Ali Farhadi. "YOLO9000: better, faster, stronger". In: *CVPR*. 2017, pp. 7263–7271.

[107] Joseph Redmon et al. "You only look once: Unified, real-time object detection". In: *CVPR*. 2016, pp. 779–788.

[108] Shaoqing Ren et al. "Faster r-cnn: Towards real-time object detection with region proposal networks". In: *NeurIPS* 28 (2015).

[109] Jamie D Roitman and Michael N Shadlen. "Response of neurons in the lateral intraparietal area during a combined visual discrimination reaction time task". In: *J NEUROSCI* 22.21 (2002), pp. 9475–9489.

[110] Hadi Salman et al. "Certified patch robustness via smoothed vision transformers". In: *CVPR*. 2022, pp. 15137–15147.

[111] Takami Sato et al. "Dirty road can attack: Security of deep learning based automated lane centering under {Physical-World} attack". In: *USENIX Security*. 2021, pp. 3309–3326.

[112] Athena Sayles et al. "Invisible perturbations: Physical adversarial examples exploiting the rolling shutter effect". In: *CVPR*. 2021, pp. 14666–14675.

[113] Mahmood Sharif et al. "A general framework for adversarial examples with objectives". In: *ACM TOPS* 22.3 (2019), pp. 1–30.

[114] Mahmood Sharif et al. "Accessorize to a crime: Real and stealthy attacks on state-of-the-art face recognition". In: *ACM SIGSAC*. 2016, pp. 1528–1540.

[115] Hocheol Shin et al. "Illusion and dazzle: Adversarial optical channel exploits against lidars for automotive applications". In: *CHES*. 2017, pp. 445–467.

[116] Inderjeet Singh et al. "On brightness agnostic adversarial examples against face recognition systems". In: *BIOSIG*. IEEE. 2021, pp. 1–5.

[117] Chawin Sitawarin et al. "Rogue signs: Deceiving traffic sign recognition with malicious ads and logos". In: *arXiv preprint:1801.02780* (2018).

[118] Dawn Song et al. "Physical adversarial examples for object detectors". In: *WOOT* 18. 2018.

[119] Rolf Sprengel, Karl Rohr, and H. Stiehl. "Thin-plate spline approximation for image registration". In: May 1998, 1190–1191 vol.3. ISBN: 0-7803-3811-1.

[120] David Strong and Tony Chan. "Edge-preserving and scale-dependent properties of total variation regularization". In: *Inverse problems* 19.6 (2003), S165.

[121] Jiachen Sun et al. "Towards robust {LiDAR-based} perception in autonomous driving: General black-box adversarial sensor attack and countermeasures". In: *USENIX Security*. 2020, pp. 877–894.

[122] Naufal Suryanto et al. "DTA: Physical Camouflage Attacks using Differentiable Transformation Network". In: *CVPR*. 2022, pp. 15305–15314.

[123] Simen Thys, Wiebe Van Ranst, and Toon Goedemé. "Fooling automated surveillance cameras: adversarial patches to attack person detection". In: *CVPR workshops*. 2019, pp. 0–0.

[124] Tzungyu Tsai et al. "Robust adversarial objects against deep learning models". In: *AAAI*. Vol. 34. 01. 2020, pp. 954–962.

[125] James Tu et al. "Physically realizable adversarial examples for lidar object detection". In: *CVPR*. 2020, pp. 13716–13725.

[126] Tomás F Yago Vicente et al. "Large-scale training of shadow detectors with noisily-annotated shadow examples". In: *ECCV*. Springer. 2016, pp. 816–832.

[127] Pradnya A Vikhar. "Evolutionary algorithms: A critical review and its future prospects". In: *ICGTSPICC*. IEEE. 2016, pp. 261–265.

[128] Jiakai Wang et al. "Dual attention suppression attack: Generate adversarial camouflage in physical world". In: *CVPR*. 2021, pp. 8565–8574.

[129] Qiang Wang et al. "Fast online object tracking and segmentation: A unifying approach". In: *CVPR*. 2019, pp. 1328–1338.

[130] Zhibo Wang et al. "advPattern: physical-world attacks on deep person re-identification via adversarially transformable patterns". In: *ICCV*. 2019, pp. 8341–8350.

[131] Hui Wei et al. "Physical Adversarial Attack meets Computer Vision: A Decade Survey". In: *arXiv preprint arXiv:2209.15179* (2022).

[132] Xingxing Wei, Ying Guo, and Jie Yu. "Adversarial Sticker: A Stealthy Attack Method in the Physical World". In: *IEEE T-PAMI* (2022).

[133] Xingxing Wei et al. "Generating Transferable Adversarial Patch by Simultaneously Optimizing its Position and Perturbations". In: (2021).

[134] Yuxin Wen et al. "Geometry-aware generation of adversarial point clouds". In: *IEEE T-PAMI* (2020).

[135] Rey Reza Wiyatno and Anqi Xu. "Physical adversarial textures that fool visual object tracking". In: *ICCV*. 2019, pp. 4822–4831.

[136] Eric Wong and Zico Kolter. "Provable defenses against adversarial examples via the convex outer adversarial polytope". In: *ICML*. 2018, pp. 5286–5295.

[137] Tong Wu, Liang Tong, and Yevgeniy Vorobeychik. "Defending against physically realizable attacks on image classification". In: *arXiv preprint v:1909.09552* (2019).

[138] Tong Wu et al. "Physical adversarial attack on vehicle detector in the carla simulator". In: *arXiv:2007.16118* (2020).

[139] Xugang Wu et al. "STA: Adversarial attacks on Siamese trackers". In: *arXiv:1909.03413* (2019).

[140] Zuxuan Wu et al. "Making an invisibility cloak: Real world adversarial attacks on object detectors". In: *ECCV*. 2020, pp. 1–17.

[141] Chong Xiang et al. "{PatchGuard}: A Provably Robust Defense against Adversarial Patches via Small Receptive Fields and Masking". In: *USENIX Security*. 2021, pp. 2237–2254.

[142] Zihao Xiao et al. "Improving transferability of adversarial patches on face recognition with generative models". In: *CVPR*. 2021, pp. 11845–11854.

[143] Cihang Xie et al. "Improving transferability of adversarial examples with input diversity". In: *CVPR*. 2019, pp. 2730–2739.

[144] Kaidi Xu et al. "Adversarial t-shirt! evading person detectors in a physical world". In: *ECCV*. 2020, pp. 665–681.

[145] Mingfu Xue et al. "NaturalAE: Natural and robust physical adversarial examples for object detectors". In: *JISA 57* (2021), p. 102694.

[146] Koichiro Yamanaka et al. "Adversarial patch attacks on monocular depth estimation networks". In: *IEEE Access* 8 (2020), pp. 179094–179104.

[147] Xiyu Yan et al. "Hijacking Tracker: A Powerful Adversarial Attack on Visual Tracking". In: *ICASSP*. IEEE. 2020, pp. 2897–2901.

[148] Jianwei Yang et al. "Embodied visual recognition". In: *arXiv:1904.04404* (2019).

[149] Kaichen Yang et al. "Beyond digital domain: Fooling deep learning based recognition system in physical world". In: *AAAI*. Vol. 34. 01. 2020, pp. 1088–1095.

[150] Maksym Yatsura et al. "Certified Defences Against Adversarial Patch Attacks on Semantic Segmentation". In: *arXiv:2209.05980* (2022).

[151] Bangjie Yin et al. "Adv-makeup: A new imperceptible and transferable attack on face recognition". In: *arXiv:2105.03162* (2021).

[152] Yang Zhang, PD Hassan Foroosh, and Boqing Gong. "CAMOU: Learning A Vehicle Camouflage For Physical Adversarial Attack On Object Detections In The Wild". In: *ICLR* (2019).

[153] Zhanyuan Zhang et al. "Clipped bagnet: Defending against sticker attacks with clipped bag-of-features". In: *2020 SPW*. IEEE. 2020, pp. 55–61.

[154] Yiqi Zhong et al. "Shadows can be Dangerous: Stealthy and Effective Physical-world Adversarial Attack by Natural Phenomenon". In: *arXiv:2203.03818* (2022).

[155] Zhe Zhou et al. "Invisible mask: Practical attacks on face recognition with infrared". In: *arXiv preprint:1803.04683* (2018).

[156] Xiaopei Zhu et al. "Fooling thermal infrared pedestrian detectors in real world using small bulbs". In: *AAAI*. Vol. 35. 4. 2021, pp. 3616–3624.

[157] Xiaopei Zhu et al. "Infrared Invisible Clothing: Hiding from Infrared Detectors at Multiple Angles in Real World". In: *CVPR*. 2022, pp. 13317–13326.

[158] Alon Zolfi et al. "The translucent patch: A physical and universal attack on object detectors". In: *CVPR*. 2021, pp. 15232–15241.